JMEPEG (2011) 20:1536–1543
DOI: 10.1007/s11665-011-9857-8

1059-9495/$19.00

THz Dielectric Properties of High Explosives Calculated by Density Functional Theory for the Design of Detectors

A. Shabaev, S.G. Lambrakos, N. Bernstein, V. Jacobs, and D. Finkenstadt

(Submitted October 29, 2010)

The current need for better detection of explosive devices has imposed a new necessity for determining the dielectric response properties of energetic materials with respect to electromagnetic wave excitation. Among the range of different frequencies for electromagnetic excitation, the THz frequency range is of particular interest because of its nondestructive nature and ability to penetrate materials that are characteristic of clothing. Typically, the dielectric response properties for electromagnetic wave excitation at THz frequencies, as well as at other frequencies, are determined by means of experimental measurements. The present study, however, emphasizes that density functional theory (DFT), and associated software technology, is sufficiently mature for the determination of dielectric response functions, and actually provides complementary information to that obtained from experiment. In particular, these dielectric response functions provide quantitative initial estimates of spectral response features that can be adjusted with respect to additional information such as laboratory measurements and other types of theory-based calculations, as well as providing for the molecular level interpretation of response structure. This point is demonstrated in the present study by calculations of ground-state resonance structure associated with the high explosives RDX, TNT1, and TNT2 using DFT, which is for the construction of parameterized dielectric response functions for excitation by electromagnetic waves at frequencies within the THz range. The DFT software NRLMOL was used for the calculations of ground-state resonance structure presented here.

Keywords advanced characterization, modeling processes, nondestructive testing

1. Introduction

In the past, quantitative understanding of the dielectric response properties of high explosives with respect to electromagnetic wave excitation was important for the purposes of monitoring munitions stockpiles under control of the US Navy and similar defense-related organizations. This was necessary in that stored explosives are typically characterized by shelf lives and tend to degrade with time, as well as being subject to environmental influences associated with storage, which can contribute to either their degradation or instability. In addition to understanding the dielectric response of individual explosives, as pure systems, it was necessary to understand their dielectric response as a component of a layered composite material. This was necessary in that many explosives, as used in practice, are a composite of binding material, whose purpose can be both chemical and structural. It follows that, in the past, a primary motivation for quantitative understanding of dielectric properties of high explosives was for the purposes accessing energetic materials performance. The current need for better detection of explosive devices, however, has imposed a new motivation for quantitative understanding of dielectric response properties of high explosives with respect to electromagnetic wave excitation. This motivation is the goal of better detecting improvised explosive devices (IEDs), which is in contrast to the goal of better accessing the materials performance of industrially fabricated explosives for munitions purposes.

Among the range of different frequencies for electromagnetic excitation, for the purposes of IED detection, the THz frequency range is of particular interest because of its nondestructive nature and ability to penetrate materials that are characteristic of clothing. Typically, the dielectric response properties for electromagnetic wave excitation at THz frequencies, as well as at other frequencies, are determined by means of experimental measurements. The present study, however, emphasizes that density functional theory (DFT), and associated software technology, is sufficiently mature for the determination of dielectric response functions, and actually provides complementary information to that obtained from experiment. In particular, these dielectric response functions provide quantitative initial estimates of spectral response features that can be adjusted with respect to additional information such as laboratory measurements and other types of theory-based calculations, as well as providing for the molecular level interpretation of response structure.

A significant aspect of using response spectra calculated by DFT for the direct construction of permittivity functions is that it adopts the perspective of computational physics, according to which a numerical simulation represents another source of ''experimental'' data. This perspective is significant in that a general procedure may be developed for construction of permittivity functions using DFT calculations as a quantitative initial estimate of spectral response features for subsequent

A. Shabaev, George Mason University, Fairfax, VA; **S.G. Lambrakos, N. Bernstein,** and **V. Jacobs**, Naval Research Laboratory, Washington, DC; and **D. Finkenstadt**, U.S. Naval Academy, Annapolis, MD. Contact e-mail: lambrakos@anvil.nrl.navy.mil.

adjustment with respect to additional information. That is to say, for the purpose of simulating many electromagnetic response characteristics of materials, DFT is sufficiently mature for the purpose of generating data complementing, as well as superseding, experimental measurements.

In the case of THz excitation of materials, the procedure of using response spectra calculated using DFT for the direct construction of permittivity functions is well posed owing to the physical characteristic of THz excitation. In particular, it is important to note that the procedure for constructing a permittivity function using response spectra calculated by DFT is physically consistent with the characteristically linear response associated with THz excitation of molecules. Accordingly, one observes a correlation between the advantages of using THz excitation for detection of IEDs (and ambient materials) and those for its numerical simulation based on DFT. Specifically, THz excitation is associated with frequencies that are characteristically perturbative to molecular states, in contrast to frequencies that can induce appreciable electronic state transitions. Of course, the practical aspect of the perturbative character of THz excitation for detection is that detection methodologies can be developed which do not damage materials under examination. The perturbative character of THz excitation with respect to molecular states has significant implications with respect to its numerical simulation based on DFT. It follows then that, owing to the perturbative character of THz excitation, which is characteristically linear, one is able to make a direct association between local oscillations about ground-state minima of a given molecule and THz excitation spectra.

In what follows, calculations are presented of ground-state resonance structure associated with the high explosives RDX, TNT1, and TNT2 using DFT. This resonant structure is for the construction of parameterized dielectric response functions for excitation by electromagnetic waves at compatible frequencies. For this purpose, the DFT software NRLMOL was adopted (Ref 1-7).

The organization of the subject areas presented here are as follows. First, a general review of the elements of DFT relevant for the calculation of absorption spectra is presented. This review focuses on the specific numerical implementation of DFT, which is embodied by the NRLMOL software. Second, a general review is presented concerning the formal structure of permittivity functions in terms of analytic function representations. An understanding of the formal structure of permittivity functions in terms of both physical consistency and causality is important for postprocessing of DFT calculations for the purpose of constructing permittivity functions. Third, information concerning the ground-state resonance structure of the explosives RDX, TNT1, and TNT2, which is obtained using DFT, is presented as a set of case studies. This information consists of the ground-state molecular geometry and response spectrum for an isolated molecule. In addition, for each of the explosives, a prototype calculation is presented to demonstrate the construction of parameterized permittivity functions using response spectra calculated using DFT. Fourth, a discussion is presented that elucidates the utility of the information concerning the ground-state resonance structure of the explosives considered. This discussion also indicates the relevance of this information for the construction of permittivity functions for frequencies that exceed the THz regime. Finally, a conclusion is given, indicating possible future pathways for extension of the methodology presented and the calculation of spectra for other molecular systems.

2. Construction of Permittivity Functions Using DFT

2.1 Density Functional Theory

The application of DFT and related methodologies for the determination of electromagnetic response characteristics is important for the analysis of parameter sensitivity. That is to say, many characteristics of the electromagnetic response of a given material may not be detectable, or in general, not relevant for detection. Accordingly, sensitivity analyses concerning the electromagnetic response of layered composite systems can adopt the results of simulations using DFT, and related methodologies, to provide realistic limits on detectability that are independent of a specific system design for IED detection. In addition, analysis of parameter sensitivity based on atomistic response characteristics of a given material, obtained by DFT, provide for an "optimal" best fit of experimental measurements for the construction of permittivity functions. It follows that within the context of parameter sensitivity analysis, data obtained by means of DFT represents a true complement to data that has been obtained by means of experimental measurements.

The NRLMOL software can be used to compute an approximation of the IR absorption spectrum of a molecule (Ref 1-7). NRLMOL uses DFT to compute the ground-state electronic structure in the Born-Oppenheimer approximation using Kohn-Sham DFT (Ref 8-10). NRLMOL uses a Gaussian orbital basis to describe the electronic wavefunctions and density, with numerical integration that is nearly exact to machine precision. For a given set of nuclear positions, the calculation directly gives the electronic charge density of the molecule, the total energy E, and the forces on each atom

$$F_\alpha^i = \frac{\partial E}{\partial r_\alpha^i}, \qquad \text{(Eq 1)}$$

where r_α^i is the α cartesian component of the position of atom i and F_α^i is the corresponding force. The dipole moment of the molecule is easily computed from the combined (nuclear and electronic) charge density.

To compute the minimum energy atomic configuration, NRLMOL uses the conjugate-gradient algorithm (Ref 11). The vibrational spectrum depends on the atomic mass matrix $M_{i\alpha j\beta} = \delta_{ij}\delta_{\alpha\beta}m_i$, where m_i is the mass of atom i and the energy second derivative matrix

$$D_{i\alpha j\beta} = \frac{\partial^2 E}{\partial r_\alpha^i \partial r_\beta^j} \qquad \text{(Eq 2)}$$

through the eigenproblem

$$\sum_{j\beta} \left(D_{i\alpha j\beta} - \varepsilon_n M_{i\alpha j\beta}\right) X_{j\beta}^{(n)} = 0. \qquad \text{(Eq 3)}$$

The generalized eigenvalues ε_n are the squares of the vibrational frequencies $\omega_n = 2\pi c\nu_n$, and the eigenvectors $X_{j\beta}^{(n)}$ give the corresponding atomic displacements:

$$\Delta r_{j\beta} = \sum_n Q_n \cdot X_{j\beta}^{(n)}, \qquad \text{(Eq 4)}$$

where Q_n is the normal mode coordinate. The eigenvectors are normalized according to the condition

$$\sum_{i\alpha,j\beta} X_{i\alpha}^{(m)} M_{i\alpha j\beta} X_{j\beta}^{(n)} = \delta_{mn}. \qquad \text{(Eq 5)}$$

NRLMOL computes the energy second derivatives Eq 2 by finite differences, computing the forces for displacement perturbations of each atom along each Cartesian direction. The first derivatives of the dipole moment with respect to atomic positions $\partial\vec{\mu}/\partial r_{\alpha}^{i}$ are also computed at the same time. Each vibrational eigenmode leads to one peak in the absorption spectrum, at a frequency equal to the mode's eigenfrequency. It is significant to note, however, that the finite-difference energy second derivatives represent an approximation of the exact second derivatives and a correction that reduces the associated error of this approximation is obtained by directly recomputing the second derivatives of the energy with respect to the eigenvectors displacements.

The absorption intensity corresponding to a particular eigenmode for a single molecule is given by

$$I_n = \frac{\pi}{3c}\left|\frac{d\vec{\mu}}{dQ_n}\right|^2, \qquad \text{(Eq 6)}$$

where c is the speed of light in a vacuum, and

$$\frac{d\vec{\mu}}{dQ_n} = \sum_{\alpha i}\frac{\partial\vec{\mu}}{\partial r_{\alpha}^{i}}X_{i\alpha}^{(n)}. \qquad \text{(Eq 7)}$$

The intensity Eq 6 must then be multiplied by the number density of molecules to give an absorption strength. It follows that the absorption spectrum calculated by NRLMOL is a sum of delta functions whose positions and magnitudes correspond to the vibrational frequencies and magnitudes, respectively. In principle, however, these spectral components must be broadened and shifted to account for anharmonic effects such as finite mode lifetimes and inter-mode couplings.

2.1.1 Remark. The ground-state resonance modes calculated by NRLMOL, which are commensurate with electromagnetic wave excitation at THz frequencies, follow a "frozen phonon" type method. This method entails numerically a predictor-corrector procedure.

2.2 Dielectric Permittivity Functions

The general approach of constructing permittivity functions according to the best fit of available data for given material corresponding to many different types of experimental measurements has been typically the dominant approach, e.g., the permittivity function of water. The general framework presented here considers an extension of this approach in that calculations of electromagnetic response based on DFT is also adopted as data for construction of permittivity functions. The inclusion of this type of information is significant for accessing what spectral response features at the molecular level are actually detectable with respect to a given set of detection parameters. Accordingly, permittivity functions having been constructed using DFT calculations provide a quantitative correlation between macroscopic material response and molecular structure. Within this context, it is not important that the permittivity function be quantitatively accurate for the purpose of being adopted as input for system simulation. Rather, it is important that permittivity function be qualitatively accurate in terms of specific dielectric response features for the purpose of sensitivity analysis, which is relevant for the assessment of absolute detectability of different types of molecular structure with respect to a given set of detection parameters. That is to say, permittivity functions that have been determined using DFT can provide a mechanistic interpretation of material response to electromagnetic excitation that could establish the well-posedness of a given detection methodology for detection of specific molecular characteristics. Within the context of practical application, permittivity functions having been constructed according to the best fit of available data would be "correlated" with those obtained using DFT for proper interpretation of permittivity-function features. Subsequent to establishment of good correlation between DFT and experiment, DFT calculations can be adopted as constraints for the purpose of constructing permittivity functions, whose features are consistent with molecular level response, for adjustment relative to specific sets of either experimental data or additional molecular level information.

The construction of permittivity functions using DFT calculations involves, however, an aspect that requires serious consideration. This aspect concerns the fact that a specific parametric function representation must be adopted. Accordingly, any parametric representation, i.e., parameterization, adopted for permittivity-function construction must be physically consistent with specific molecular response characteristics, while limiting the inclusion of feature characteristics that tend to mask response signatures that may be potentially detectable.

In principle, parameterizations are of two classes. One class consists of parameterizations that are directly related to molecular response characteristics. This class of parameterizations would include spectral scaling and width coefficients. The other class consists of parameterizations that are purely phenomenological and are structured for optimal and convenient best fits to experimental measurements. A sufficiently general parameterization of permittivity functions is given by Drude-Lorentz approximation (Ref 12, 13)

$$\varepsilon(\nu) = \varepsilon'(\nu) + i\varepsilon''(\nu) = \varepsilon_{\infty} + \sum_{n=1}^{N}\frac{\nu_{np}^2}{(\nu_{no}^2 - \nu^2) - i\gamma_n\nu}, \qquad \text{(Eq 8)}$$

where ν_{np} and γ_n are the spectral scaling and width of a resonance contributing to the permittivity function. The permittivity ε_{∞} is a constant since the dielectric response at high frequencies is substantially detuned from the probe frequency. The real $\varepsilon_r(\nu)$ and imaginary $\varepsilon_i(\nu)$ parts of the permittivity function can be written separately as

$$\varepsilon_r(\nu) = \varepsilon_{\infty} + \sum_{n=1}^{N}\frac{\nu_{np}^2(\nu_{no}^2 - \nu^2)}{(\nu_{no}^2 - \nu^2)^2 + \gamma_n^2\nu^2} \quad \text{and}$$
$$\varepsilon_i(\nu) = \sum_{n=1}^{N}\frac{\nu_{np}^2\gamma_n\nu}{(\nu_{no}^2 - \nu^2)^2 + \gamma_n^2\nu^2}. \qquad \text{(Eq 9)}$$

With respect to practical application, the absorption coefficient α and index of refraction n_r, given by

$$\alpha = \frac{4\pi\nu}{\sqrt{2}}\left[-\varepsilon_r + \sqrt{\varepsilon_r^2 + \varepsilon_i^2}\right]^{1/2} \quad \text{and} \quad n_r = \frac{1}{\sqrt{2}}\left[\varepsilon_r + \sqrt{\varepsilon_r^2 + \varepsilon_i^2}\right]^{1/2}, \qquad \text{(Eq 10)}$$

respectively, provide direct relationships between calculated quantities obtained by DFT and "conveniently measurable" quantities α and n_r.

3. Case Studies Demonstrating the Calculation of Dielectric Response Functions of High Explosives in Using DFT

Presented in this section are a series of case studies that demonstrate the calculation of dielectric response functions for the THz range of frequencies using DFT. These case studies consider the dielectric response of the high explosives RDX, TNT1, and TNT2. In each case study, two sets of data are presented, which are the results of computational experiments using DFT. These are the relaxed or equilibrium configurations of isolated molecules and ground-state oscillation frequencies and IR intensities for these configurations that are calculated by DFT according to the frozen phonon approximation.

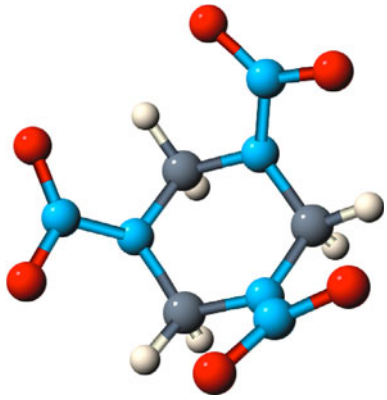

Fig. 1 Molecular geometry of RDX

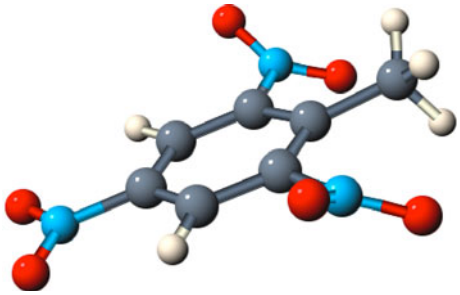

Fig. 2 Molecular geometry of TNT1

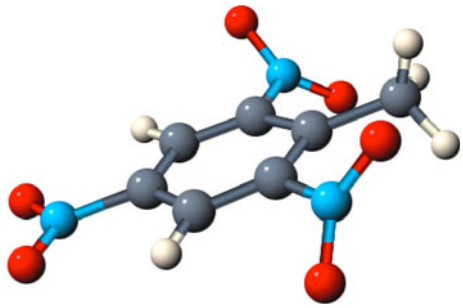

Fig. 3 Molecular geometry of TNT2

A schematic representation of the molecular geometries of RDX, TNT1, and TNT2 are shown in Fig. 1, 2, and 3, respectively. The atomic positions of the equilibrium configurations of RDX, TNT1, and TNT2 calculated using DFT are shown in Table 1, 2, and 3, respectively. Shown in Fig. 4, 5, and 6 are the IR intensities as a function of frequency calculated using DFT for RDX, TNT1, and TNT2, respectively, according to a frozen phonon approximation. For the spectra shown in these figures, the forms of the resonance responses are approximated essentially by delta functions. The oscillation frequencies and IR intensities calculated using DFT for RDX, TNT1, and TNT2 are shown in Table 4, 5, and 6, respectively.

The DFT calculated absorption spectra shown in Table 4, 5, and 6 provide two types of information for general analysis of dielectric response. These are the denumeration of ground-state resonance modes and estimates of molecular level dielectric response structure. The construction of permittivity functions using the DFT-calculated absorption spectra follows the same procedure as that applied for the construction of permittivity functions using experimentally measured absorption spectra, but with the addition of certain constraint conditions. These constraint conditions being a priori fixed locations of the resonance modes. Accordingly, construction of permittivity functions using either DFT or experimentally measured absorption spectra requires parameterizations that are in terms of physically consistent analytic function representations such as the Drude-Lorentz model. Although the formal structure of permittivity functions constructed using DFT and experimental measurements are the same, their interpretation with respect to parameterization is different for each case.

The construction of permittivity functions using experimental measurements, an established methodology, defines an

Table 1 Atomic positions for equilibrium configuration of RDX (Å)

Atomic number	*X*	*Y*	*Z*	Atomic number	*X*	*Y*	*Z*
7	1.16994	−0.81313	0.09076	8	−1.12995	1.87973	2.52487
7	0.09076	1.16994	−0.81313	8	3.34946	−0.19764	0.06923
7	−0.81313	0.09076	1.16994	8	0.06923	3.34946	−0.19764
7	2.44674	−0.67765	0.7438	8	−0.19764	0.06923	3.34946
7	0.7438	2.44674	−0.67765	1	−1.50333	1.88316	0.33719
7	−0.67765	0.7438	2.44674	1	0.33719	−1.50333	1.88316
6	−1.09011	0.92662	0.00735	1	1.88316	0.33719	−1.50333
6	0.00735	−1.09011	0.92662	1	−1.82611	0.39667	−0.61584
6	0.92662	0.00735	−1.09011	1	−0.61584	−1.82611	0.39667
8	2.52487	−1.12995	1.87973	1	0.39667	−0.61584	−1.82611
8	1.87973	2.52487	−1.12995				

Table 2 Atomic positions for equilibrium configuration of TNT1 (Å)

Atomic number	X	Y	Z	Atomic number	X	Y	Z
1	1.277	−0.71765	1.9543	6	1.41827	−0.47815	−2.75813
1	−2.49724	−0.7602	−0.12405	7	−1.38812	−0.82281	2.33281
1	0.77359	−0.73572	−3.60038	7	2.83728	−0.47406	−0.14338
1	2.29092	−1.14373	−2.77796	7	−1.56142	−0.74062	−2.57029
1	1.80338	0.54246	−2.88489	8	3.37643	0.34145	−0.89378
6	0.71266	−0.68704	1.02471	8	3.41117	−1.19787	0.67094
6	−0.67498	−0.7428	1.03277	8	−0.69699	−0.7987	3.35263
6	−1.40976	−0.72761	−0.14562	8	−2.61686	−0.90672	2.29484
6	−0.71255	−0.68459	−1.3493	8	−2.49644	0.05804	−2.62488
6	0.69021	−0.58801	−1.44921	8	−1.28456	−1.59556	−3.41343
6	1.35505	−0.58239	−0.20393				

Table 3 Atomic positions for equilibrium configuration of TNT2 (Å)

Atomic number	X	Y	Z	Atomic number	X	Y	Z
1	1.277	−0.71765	1.9543	6	1.41827	−0.47815	−2.75813
1	−2.49724	−0.7602	−0.12405	7	−1.38812	−0.82281	2.33281
1	0.77359	−0.73572	−3.60038	7	2.83728	−0.47406	−0.14338
1	2.29092	−1.14373	−2.77796	7	−1.56142	−0.74062	−2.57029
1	1.80338	0.54246	−2.88489	8	3.37643	0.34145	−0.89378
6	0.71266	−0.68704	1.02471	8	3.41117	−1.19787	0.67094
6	−0.67498	−0.7428	1.03277	8	−0.69699	−0.7987	3.35263
6	−1.40976	−0.72761	−0.14562	8	−2.61686	−0.90672	2.29484
6	−0.71255	−0.68459	−1.3493	8	−2.49644	0.05804	−2.62488
6	0.69021	−0.58801	−1.44921	8	−1.28456	−1.59556	−3.41343
6	1.35505	−0.58239	−0.20393				

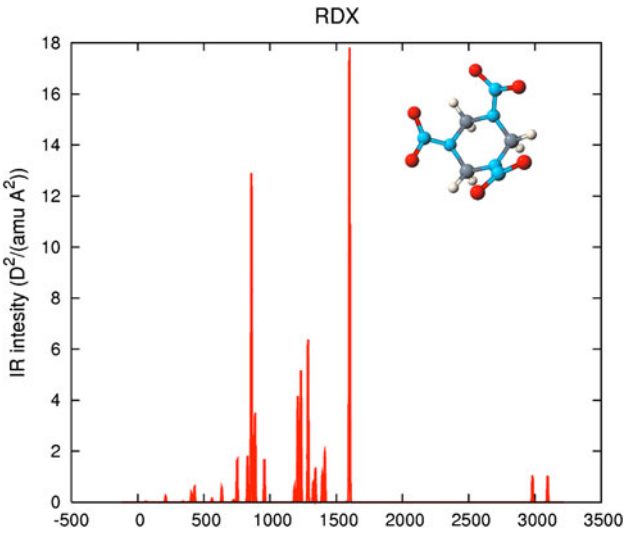

Fig. 4 IR intensity as a function of frequency calculated using DFT for RDX according to frozen phonon approximation

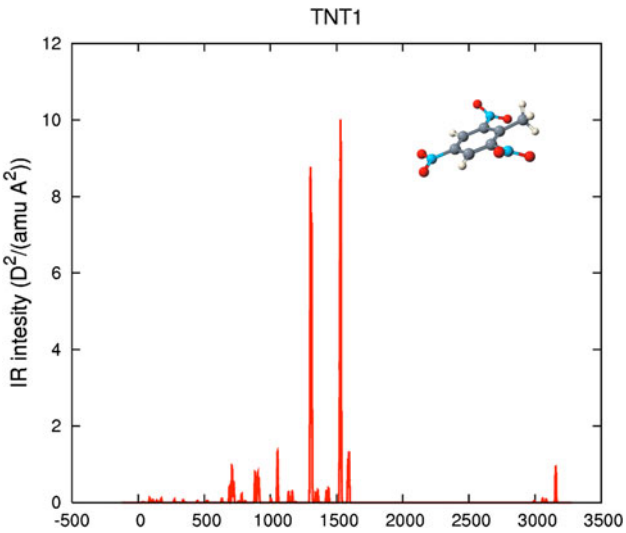

Fig. 5 IR intensity as a function of frequency calculated using DFT for TNT1 according to frozen phonon approximation

inverse problem where resonant locations, peaks and widths, as well as the number of resonances, are assumed adjustable. Following this approach, it follows that many of the detailed characteristics of resonance structure are smoothed or averaged. In addition, measurement artifacts associated with sample preparation and detector configuration can in principle introduce errors. One advantage of permittivity functions constructed using experimental measurements, however, is that many aspects of dielectric response on the macroscale that are associated with multiscale averaging and molecule-lattice coupling are taken into account inherently. Accordingly, the disadvantage of this approach is that the nature of any multiscale averaging and resonant structure, contributing to dielectric response on the macroscopic level, may not be

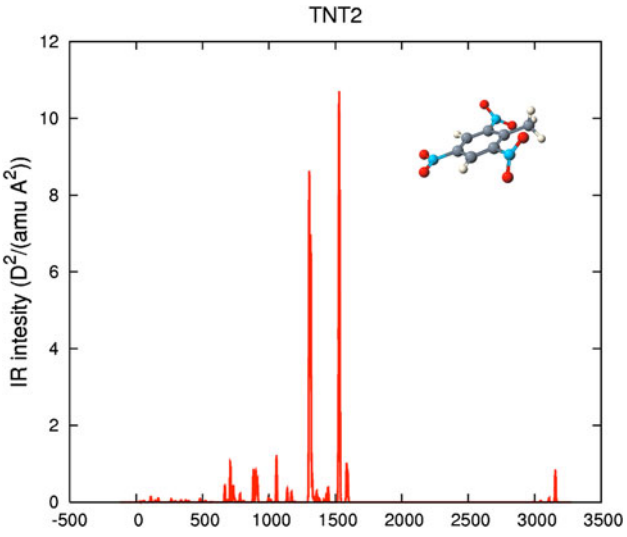

Fig. 6 IR intensity as a function of frequency calculated using DFT for TNT2 according to frozen phonon approximation

understood. This lack of quantitative understanding of microscale response structure, as it would occur without the multiscale averaging associated with macroscale response structure, can in principle inhibit the development of pump-probe type methodologies for selective excitation of molecular modes, or the development of filter algorithms, which are for the purpose of enhanced signature detection or modulation.

The construction of permittivity functions using DFT calculations, the methodology whose development is considered here, defines a direct problem approach where dielectric response is estimated within the bounds of relatively well-defined adjustable parameters. Following this approach, a permittivity function is constructed using the DFT-calculated absorption spectra, e.g., Table 4, 5, and 6, under the condition that the calculated resonance locations are fixed, while resonance widths and number densities are assumed adjustable, e.g., Fig. 7, 8, and 9. Better interpretation of dielectric response of explosives on a macroscale can be achieved through correlation of resonance structure that is experimentally observed and that which is calculated by DFT. In principle, correlation of resonance structure would include the quantitative

Table 4 Oscillation frequencies and IR intensities for RDX

Frequency, cm^{-1}	Intensity, D^2/(amu Å^2)	Frequency, cm^{-1}	Intensity, D^2/(amu Å^2)	Frequency, cm^{-1}	Intensity, D^2/(amu Å^2)	Frequency, cm^{-1}	Intensity, D^2/(amu Å^2)
50.4476	0.0012	561.592	0.068	958.8454	0.841	1394.1574	0.5447
51.1589	0.0012	561.6381	0.0682	958.8824	0.8369	1395.0201	0.5394
77.7345	0.0128	573.1913	0.0001	1106.4304	0	1414.4218	1.9899
91.1576	0.0081	635.6372	0.2794	1185.1197	0.598	1572.3865	0.0002
125.232	0.0004	635.8515	0.2799	1208.9255	2.0878	1600.7625	8.9248
125.1679	0.0004	723.8626	0.0454	1209.0906	2.0855	1600.6959	8.9225
215.3785	0.1185	728.3136	0.0363	1218.0051	0.0005	2979.9541	0.0238
215.3755	0.1184	728.3277	0.036	1231.9493	2.5768	2980.1722	0.0204
290.8681	0.0001	752.231	1.6486	1231.8716	2.5783	2983.6473	1.0283
346.3176	0.0151	830.6969	0.908	1284.8248	6.3921	3098.3191	0.3366
346.2359	0.0151	830.9032	0.9079	1304.8515	0.0003	3099.4052	0.3341
392.0173	0.0047	859.1975	6.4437	1326.7768	0.368	3096.9028	0.4219
391.356	0.0047	858.8267	6.4375	1327.4575	0.3693		
413.5828	0.3457	863.9551	0.0141	1344.0359	0.6348		
431.3056	0.5958	886.788	3.5023	1344.7081	0.6313		

Table 5 Oscillation frequencies and IR intensities for TNT1

Frequency, cm^{-1}	Intensity, D^2/(amu Å^2)	Frequency, cm^{-1}	Intensity, D^2/(amu Å^2)	Frequency, cm^{-1}	Intensity, D^2/(amu Å^2)	Frequency, cm^{-1}	Intensity, D^2/(amu Å^2)
172.5174	0.0237	414.8762	0.0385	908.0919	0.4081	1449.4697	0.2159
197.4056	0.011	495.2412	0.0797	913.9983	0.5736	1487.7755	0.4935
135.2506	0.001	522.6106	0.0393	1057.9824	0.0914	1528.3766	4.1144
284.1745	0.0427	560.2942	0.0077	1068.9096	0.1036	1524.3186	6.5037
361.7698	0.012	578.169	0.0073	1057.3348	1.2247	1532.7054	3.8635
427.1822	0.133	668.3243	0.432	1137.2714	0.3466	1585.1704	1.0497
172.7674	0.0458	702.98	0.0633	1177.5714	0.2562	1592.6665	0.7857
171.747	0.0908	709.4691	1.031	1190.6768	0.0231	2804.9617	0.0052
177.736	0.0114	733.5913	0.398	1301.8607	8.6558	2860.6966	0.0794
285.6632	0.0627	744.7193	0.1154	1308.2775	7.0606	2930.3248	0.053
300.4711	0.0241	768.8811	0.017	1325.0594	0.5661	3154.161	0.4024
304.604	0.0077	783.0319	0.2198	1355.3609	0.1079	3160.6014	0.5166
337.6068	0.0188	808.5178	0.0437	1385.5683	0.2682		
342.8559	0.0512	889.7004	0.8604	1386.0299	0.0801		
376.9598	0.053	907.8869	0.4586	1462.453	0.0542		

Table 6 Oscillation frequencies and IR intensities for TNT2

Frequency, cm^{-1}	Intensity, D^2/(amu Å^2)	Frequency, cm^{-1}	Intensity, D^2/(amu Å^2)	Frequency, cm^{-1}	Intensity, D^2/(amu Å^2)	Frequency, cm^{-1}	Intensity, D^2/(amu Å^2)
172.5174	0.0237	414.8762	0.0385	908.0919	0.4081	1449.4697	0.2159
197.4056	0.011	495.2412	0.0797	913.9983	0.5736	1487.7755	0.4935
135.2506	0.001	522.6106	0.0393	1057.9824	0.0914	1528.3766	4.1144
284.1745	0.0427	560.2942	0.0077	1068.9096	0.1036	1524.3186	6.5037
361.7698	0.012	578.169	0.0073	1057.3348	1.2247	1532.7054	3.8635
427.1822	0.133	668.3243	0.432	1137.2714	0.3466	1585.1704	1.0497
172.7674	0.0458	702.98	0.0633	1177.5714	0.2562	1592.6665	0.7857
171.747	0.0908	709.4691	1.031	1190.6768	0.0231	2804.9617	0.0052
177.736	0.0114	733.5913	0.398	1301.8607	8.6558	2860.6966	0.0794
285.6632	0.0627	744.7193	0.1154	1308.2775	7.0606	2930.3248	0.053
300.4711	0.0241	768.8811	0.017	1325.0594	0.5661	3154.161	0.4024
304.604	0.0077	783.0319	0.2198	1355.3609	0.1079	3160.6014	0.5166
337.6068	0.0188	808.5178	0.0437	1385.5683	0.2682		
342.8559	0.0512	889.7004	0.8604	1386.0299	0.0801		
376.9598	0.053	907.8869	0.4586	1462.453	0.0542		

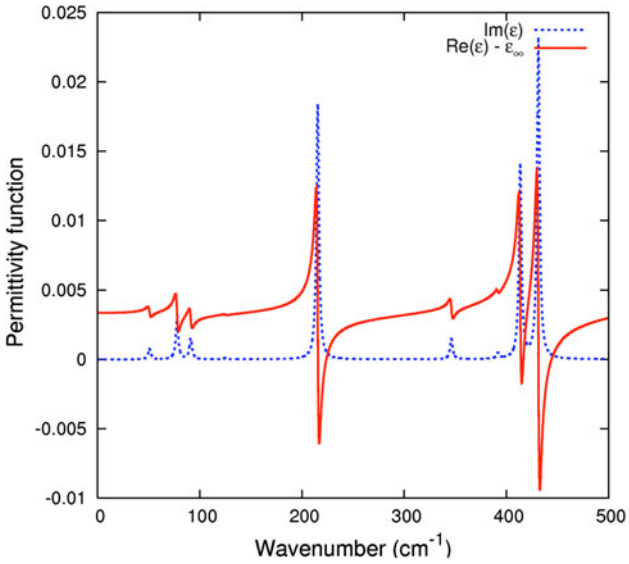

Fig. 7 Real (solid) and imaginary (dashed) parts of permittivity function of RDX molecules with $\gamma_n = 3\ cm^{-1}$ and $\rho = 2.4 \times 10^{19}\ cm^{-3}$ for frequencies within THz range

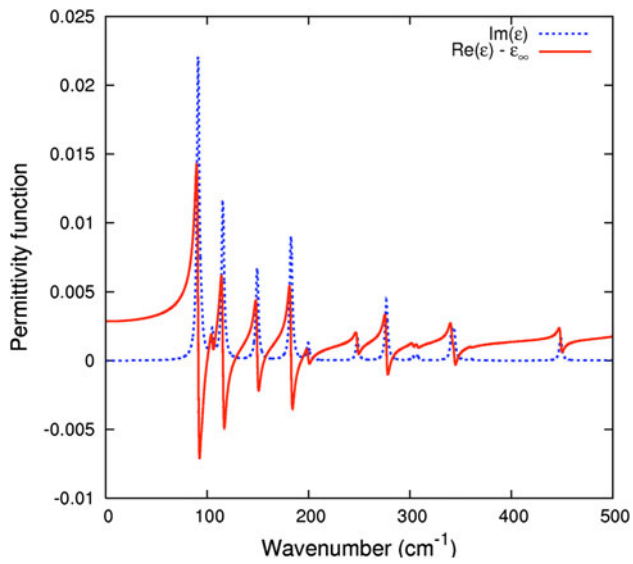

Fig. 8 Real (solid) and imaginary (dashed) parts of permittivity function of TNT1 molecules with $\gamma_n = 3\ cm^{-1}$ and $\rho = 2.4 \times 10^{19}\ cm^{-3}$ for frequencies within THz range

analysis of changes in signature features associated with the transition of the system from that of a low-density system of uncoupled molecules to that of a bulk lattice.

One purpose of DFT-calculated spectra, which is related to practical application, and extremely important for the interpretation of signature features and design of detectors, is the quantitative analysis of absolute bounds, or rather, the inherent limitation on levels of detection associated with various types of detection strategies. With respect to the purpose of examining inherent limitations on IED detection, the dominant features of response spectra that are calculated using DFT provide a foundation for establishing what level of detection is achievable in the absence of instrumental and environmental factors associated with detection. Accordingly, the approach presented here, for construction of permittivity functions, provides a specific application of DFT. For any given energetic material and frequency range of the incident electromagnetic wave, DFT can calculate a set of response signatures that are each characterized by an excitation frequency, magnitude, and width. These response signatures must then be adjusted parametrically to construct permittivity functions. Accordingly, parameter adjustment with respect to a given set of experimental measurements, which would entail parameter optimization and sensitivity analysis, will determine what types of signature structure are recoverable at the level of detection for a given detector design.

With respect to more extensive DFT calculations concerning the ground-state absorption spectra of a bulk lattice or spectra corresponding to electronic state transitions, it is important to note that the atomic positions of the relaxed or equilibrium configuration of a single isolated molecule, e.g., Table 1, 2, and 3, provide a convenient starting point. Calculation of the dielectric response of a bulk lattice would entail, in principle, the construction of a super cell consisting of molecules whose initial positions are those determined by DFT for isolated systems. Additional constraints on this super cell could be

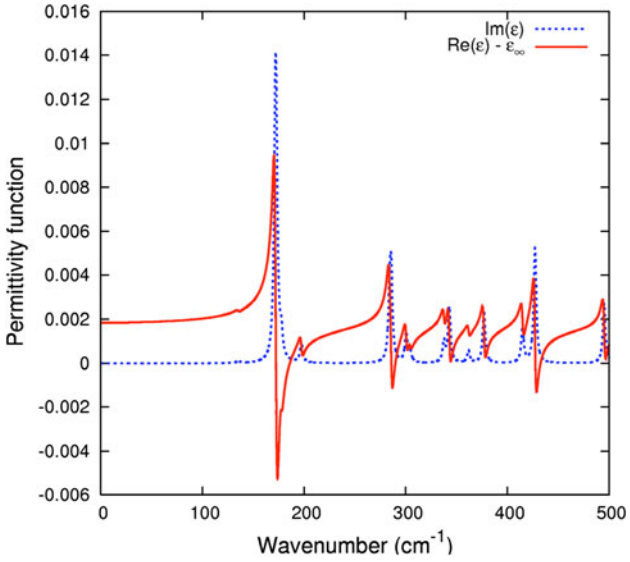

Fig. 9 Real (solid) and imaginary (dashed) parts of permittivity function of TNT2 molecules with $\gamma_n = 3\ cm^{-1}$ and $\rho = 2.4 \times 10^{19}\ cm^{-3}$ for frequencies within THz range

based on crystallographic information concerning bulk density or lattice spacing. Calculation of the dielectric response associated with electronic state transitions would entail the application of methods based on perturbation theory. In principle, for these methods most of the computational effort is expended for determination of the ground state, with respect to which all excited states are determined self-consistently. These methods typically would be based on time-dependent density functional theory (TDDFT) (Ref 14, 15).

The DFT calculations presented here were performed using the DFT software NRLMOL. With respect to the approach presented here for construction of permittivity functions, these calculations represent the result of a numerical experiment with the "numerical apparatus" NRLMOL, which has associated with it specific discrete numerical representations and associated approximations. It follows that additional numerical experiments concerning the explosives considered in this study should be conducted using other DFT software implementations. The results of these numerical experiments would in principle represent both additional information, as well as consistency checks for different DFT computer codes. Again, an underlying factor supporting the construction of permittivity functions using DFT-calculated spectra is that the associated software technology has evolved to a point of maturity where dielectric response to electromagnetic excitation can be determined quantitatively for large molecular systems.

4. Conclusion

The calculations of ground-state resonance structure associated with the high explosives RDX, TNT1, and TNT2 using DFT are meant to serve as reasonable estimates of molecular level response characteristics, providing interpretation of dielectric response features, for subsequent adjustment relative to experimental measurements and molecular structure theory. These calculations demonstrate that DFT and its associated software implementations, e.g., NRLMOL, should be viewed as a practical tool for determining quantitative estimates of dielectric response properties of high explosives. That is to say, DFT calculations should be considered as computational experiments in their own right, which provide information that is complementary to that obtained by experimental measurement of response spectra, as well as that obtained from other computational experiments, i.e., other DFT software implementations. It follows that the establishment of a general constrained parameterization of the dielectric response of explosives, based on both DFT and experiment, combined with quantitative sensitivity analyses of this parameterization, will provide an assessment of the detectability of a given explosive, independent of specific detector design.

Acknowledgment

This work was supported by the Office of Naval Research.

References

1. M.R. Pederson and K.A. Jackson, Variational Mesh for Quantum-Mechanical Simulations, *Phys. Rev. B*, 1990, **41**, p 7453
2. K.A. Jackson and M.R. Pederson, Accurate Forces in a Local-Orbital Approach to the Local-Density Approximation, *Phys. Rev. B*, 1990, **42**, p 3276
3. A. Briley, M.R. Pederson, K.A. Jackson, D.C. Patton, and D.V. Porezag, Vibrational Frequencies and Intensities of Small Molecules: All-Electron, Pseudopotential, and Mixed-Potential Methodologies, *Phys. Rev. B*, 1998, **58**, p 1786
4. D.V. Porezag and M.R. Pederson, Infrared Intensities and Raman-Scattering Activities Within Density-Functional Theory, *Phys. Rev. B*, 1996, **54**, p 7830
5. D.V. Porezag and M.R. Pederson, Optimization of Gaussian Basis Sets for Density-Functional Calculations, *Phys. Rev. A*, 1999, **60**, p 2840
6. M.R. Pederson, D.V. Porezag, J. Kortus, and D.C. Patton, Strategies for Massively Parallel Local-Orbital-Based Electronic Structure Methods, *Phys. Status Solidif. B*, 2000, **217**, p 197
7. K. Jackson, M.R. Pederson, D. Porezag, Z. Hajnal, and T. Frauenheim, Density-Functional-Based Predictions of Raman and IR Spectra for Small Si Clusters, *Phys. Rev. B*, 1997, **55**, p 2549
8. P. Hohenberg and W. Kohn, Inhomogeneous Electron Gas, *Phys. Rev.*, 1964, **136**, p B864
9. W. Kohn and L.J. Sham, Self-Consistent Equations Including Exchange and Correlation Effects, *Phys. Rev.*, 1965, **140**, p A1133
10. R.O. Jones and O. Gunnarson, The Density Functional Formalism, Its Applications and Prospects, *Rev. Mod. Phys.*, 1989, **61**, p 689
11. W.W. Hager and H. Zhang, A Survey of Nonlinear Conjugate Gradient Methods, *Pac. J. Optim.*, 2006, **2**, p 35–58
12. C.A.D. Roeser and E. Mazur, Light-Matter Interactions on Femtosecond Time Scale, *Frontiers of Optical Spectroscopy*,, NATO Science Series, Vol 168, B. Di Bartolo and O. Forte, Ed., Kluwer Academic Publishers, Dordrecht, Norwell, 2005, p 29
13. C.F. Bohren and D.R. Huffman, *Absorption and Scattering of Light by Small Particles*, Wiley-VCH Verlag, Weinheim, 2004
14. E. Runge and E.K.U. Gross, Density-Functional Theory for Time-Dependent Systems, *Phys. Rev. Lett.*, 1984, **52**, p 997–1000
15. M.A.L. Marques, C.A. Ullrich, F. Nogueira, A. Rubio, K. Burke, and E.K.U. Gross, Ed., *Time-Dependent Density Functional Theory*, Springer, Berlin, Heidelberg, 2006